CENTRIFUGE MODELLING OF UPHEAVAL BUCKLING IN SAND

WHITE D. J.[i], BAREFOOT A. J.[ii] and BOLTON M. D.[iii]

ABSTRACT

When operating at high temperature and internal pressure, initial imperfections in a cold laid pipeline can lead, through expansion and an increase in axial stress, to imperfection growth and upheaval buckling. Efficient design against upheaval buckling requires accurate prediction of soil uplift resistance. However, current design methods are based on empirical uplift factors chosen from soil classification data, and do not capture the strong influence of backfill density on uplift resistance.

A series of tests are reported, in which the pipe uplift is modelled in a 0.8 m diameter mini-drum centrifuge. A key advantage of the mini-drum centrifuge is that uplift tests can be carried out on small soil samples taken from boreholes along the pipeline length. Pipe uplift can be considered as a routine laboratory test.

The results demonstrate the strong influence of backfill density on peak uplift resistance. Observation of the failure mechanism suggests that existing design methods based on vertical slip planes are unrepresentative of the failure. Instead, a new solution is presented, which more closely represents the observed mechanism, and provides excellent correlation with the measured data of peak uplift resistance across a range of backfill densities. Design curves are presented, which require element test results as input parameters. However, upheaval buckling is an unusual example in which centrifuge models, standing alone, provide the most efficient design tool.

Key words: upheaval buckling, mini-drum centrifuge, pipeline, uplift, sand, soil-structure interaction, model test analysis

INTRODUCTION

The transmission of hot oil through a buried pipeline leads to thermal expansion. This expansion is resisted by the restraint imposed at the end connections and axial friction between the pipe and the surrounding soil. The resulting axial stress can lead to buckling.

Pipelines are often trenched and covered with backfill to avoid damage to the pipes from trawlgear or anchors, or for thermal insulation. Initial lack of straightness in a pipeline laid cold leads, through the increase of axial stress induced by heating and internal pressure, to the possibility of imperfection growth. Excessive upwards movement may cause the pipe to protrude from the trench; this phenomenon is known as upheaval buckling.

Imperfection growth or buckling can be suppressed by pipe weight or the mobilisation of soil uplift resistance. When designing against upheaval buckling, a three-dimensional analysis is carried out, using an appropriate model of one-dimensional uplift resistance. The available resistance largely determines the likelihood of buckling. Consequently the availability of an accurate model of uplift resistance is critical to the safe and economic design of pipelines (Schaminee et al., 1990).

A series of theoretical models for uplift resistance has been developed, based on different kinematic mechanisms (Nyman, 1984; Trautmann et al., 1985; Schaminee et al., 1990; Matyas and Davis, 1983). There is no generally accepted solution, and the existing database of results has not been resolved across all backfill densities (Kvalstad, 1999).

This paper describes a laboratory investigation to determine the true kinematic mechanism of pipe uplift, and measure the associated resistance. The use of a 0.8 m diameter mini-drum centrifuge allows an uplift test to be carried out on soil recovered from vibrocores taken at intervals along the route. This compares favourably with full-scale uplift tests, which require significantly more time and labour, and two orders of magnitude more soil. In comparison, the development of the centrifuge equipment described below now allows pipe uplift testing to be considered as a routine laboratory test.

BACKGROUND

Whilst upheaval buckling is a three-dimensional problem, the soil-pipe interaction can be analysed as one-dimensional uplift in the plane perpendicular to the axis of the pipe. Trautmann et al. (1985) presented a review of uplift solutions for anchors and pipes. The most widely used mechanism is the vertical slip model (Fig. 1). Peak uplift resistance per unit length, P, is defined as the sum of the dead weight of the overlying soil and the friction on the slip planes. Normalisation of Equation (1) produces a dimensionless uplift factor, F_{up}, and the expression shown in Equation (2). According to Equation (1), F_{up} is a function of the earth pressure coefficient and angle of friction.

$$P = (1 + K \tan \phi \, H/D) \, \gamma' \, HD \qquad (1)$$

$$P/\gamma'HD = (1 + K \tan \phi \, H/D) = 1 + F_{up} \, H/D \qquad (2)$$

A number of authors (Kulhawy et al., 1983; Matyas and Davis, 1983; Spangler and Handy, 1982) offer alternative design recommendations for K and ϕ individually. More recently, Trautmann et al. (1985), Schaminee et al. (1990) and Kvalstad (1999) discuss the selection of F_{up} from soil classification and density data.

Fig. 1. The vertical slip model

Data from previous laboratory tests is collated in Fig. 2. The data contains large scatter, notably with respect to density. The attempt to non-dimensionalise the uplift process remains incomplete, and a more satisfactory version of Equation (2) would feature the following parameters :

$$P/\gamma'HD = f (K, \phi, H/D, I_D) \qquad (3)$$

It is noted by Kvalstad (1999) that the low peak uplift factors associated with loose soil may indicate a different failure mechanism to that hypothesised by the vertical slip model. The flow of contractile loose sand around the pipe periphery is proposed as an alternative kinematic solution.

If the above hypothesis were correct, peak uplift would be a complex function, encompassing two failure mechanisms depending on soil state. In order to resolve this incongruity, and to establish the role of density in governing peak uplift resistance, a series of centrifuge tests was conducted, which included observation of the uplift mechanism.

Fig. 2. Normalised uplift, $P/\gamma'HD$ vs. H/D.

CENTRIFUGE MODELLING PROGRAMME

Mark II mini-drum centrifuge

If the cost and labour associated with full-scale pipe uplift tests are to be avoided, centrifuge modelling is essential. A reduced-scale (say 1 : 10) model of a pipe buried at 1 m depth will be under stresses of 0-2 kPa if the test is carried out on the lab floor. Over this stress range, friction and dilation angles vary widely, and differ significantly from those experienced at engineering stress levels. Also, since it is difficult to conduct element tests at such low stresses, it is hard to obtain reliable parameters to validate design methods.

The mini-drum centrifuge allows small-scale centrifuge tests to be carried out with short turnaround times and with minimal sample material. The centrifuge can be operated by a single user, and features an independent central turntable that can rotate at +/-100 rpm relative to the ring channel. The Mark II mini-drum centrifuge (Fig. 3) was commissioned at the Schofield Centrifuge Centre, Cambridge University Engineering Department, in 1995 and is described in more detail by Barker (1999). For further description of drum centrifuge technology, the reader is referred to Schofield (1998) and Stewart et al. (1998).
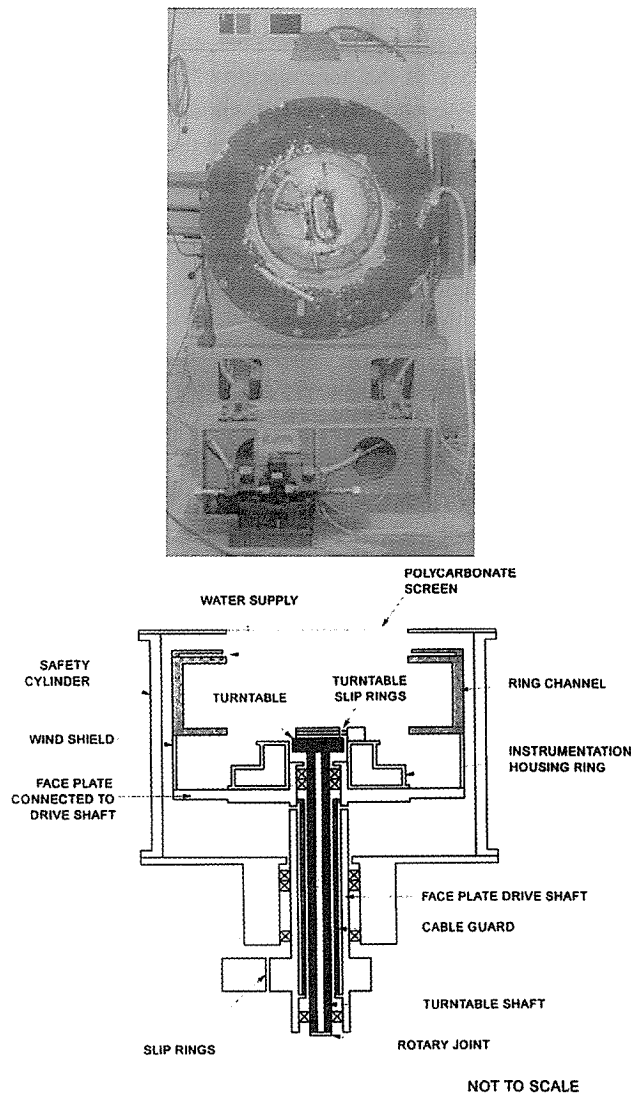
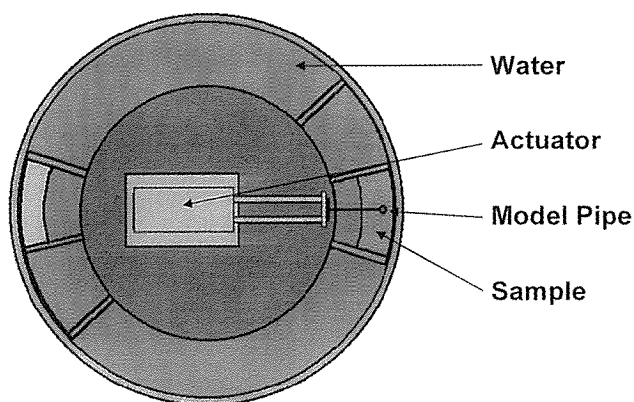Fig. 3. Mark II Mini-drum centrifuge (diagram after Barker, 1999)

Fig. 4. Schematic diagram of test apparatus

Although the mini-drum centrifuge is capable of accelerations up to 470g, these test series took place at 10g, allowing the 100 mm deep ring channel to represent a trench up to 1 m deep. A schematic diagram of the test arrangement is shown in Fig. 4. Further description can be found in Barefoot (1998).

The tests reported here were carried out with the centrifuge axis vertical so that the sum of the 10g centripetal acceleration and the 1-G acceleration due to gravity acted uniformly on the sample at all times. A test box typically contained 3 litres of soil, and was counterbalanced by a similar box across the centrifuge chamber. The net acceleration acted along a 1 in 10 incline. To ensure that the pipe is extracted parallel to this acceleration, the actuator and container are mounted at a 1 in 10 slope in the centrifuge ring channel.

Experimental Apparatus

The pullout actuator comprises a motor with a gear head linked to a lead screw to provide the necessary torque at low speeds. A servo controller, connected to the motor via the slip rings, allows the speed to be varied from outside the centrifuge whilst the test is in progress. The lead screw is attached to a cantilever load cell. The pipe hangs from the ends of the load cell and is attached by fishing wire.

The model pipe was made from brass with length 120 mm and diameter 22 mm. A linearly variable differential transformer (LVDT) was used to measure displacement.

Test Program

The tests can be divided into four series. In all the tests, the backfill material was fine sand and the initial cover depth remained constant at about 3 pipe diameters. The sample density was varied between the tests to investigate the influence of initial state on uplift resistance.

- Loose monotonic tests: L1-L4
- Dense monotonic tests: D1-D4
- Mechanism tests (medium dense): M1-M3
- Loose cyclic test: C1

The monotonic tests consisted of a simple pullout where the pipeline is lifted upwards at a rate of 5 mm/hr. This speed is sufficiently slow to ensure drained conditions (Barefoot, 1998). The mechanism tests featured coloured layers of sand, allowing displacements within the soil mass to be observed by post-test excavation. One cyclic test was carried out on a loose sample to investigate the phenomenon of uplift ratcheting over the course of several buckling cycles.

Model preparation

The material used in the tests was Fraction D silica sand supplied by David Ball Limited, Bar Hill, Cambridgeshire. Density tests revealed maximum and minimum voids ratios of 1.06 and 0.61 respectively, and the critical state angle of friction (ϕ_{crit}) was found by shear box testing to be 32°.

The loose sand samples were prepared by wet pluviation, the medium dense samples by dry pluviation, and the dense samples by dry pluviation and vibration. Each sample was constructed in a series of lifts, with regular weighings being made to ensure uniform density. The top surface was vacuumed to create a curved profile corresponding to the radial acceleration field. Saturation of the samples from the base provided sufficient suction for the samples to maintain a cliff face as the centrifuge axis was raised to the vertical. After acceleration to 10g, the centrifuge water table was slowly raised and the sample allowed to saturate fully.

Experimental results

A total of 11 tests were carried out at various relative densities. The sample properties and measured peak uplift resistance are shown in Table 1. The measured uplift factor, F_{up}, is back-calculated according to Equation (2), with due regard for the varying acceleration field throughout the depth of the sample. In each case, the normalised burial depth, H/D was 3.14.

Photographic evidence of mechanism

Tests M1-M3 used samples of identical density but were halted after pipe displacements of 5, 14 and 22 mm respectively. These correspond to displacements equal to 0.23, 0.6, and 1 pipe diameters. Post test excavation of each sample allowed the deformation of coloured marker layers to be observed. Figure 5 shows cross-sections through each excavated sample linked to the corresponding part of the uplift curves for tests M1-M3.

The repeatability of these tests is demonstrated by the similarity of the uplift curves shown in Fig. 5. The peak resistance values found in tests M1-3 have a mean of 48 N with all three tests falling within in envelope of +/- 10% of this value. Also, the shape of the uplift curve in the post-peak region is accurately repeated by tests M2 and M3. After 15 mm of displacement, these tests show a discrepancy in uplift resistance of less than 3%.

However, the pre-peak gradient of the uplift curves is slightly different, with the mobilisation distance of peak uplift varying from 2.1 mm (M1) to 2.8 mm (M2, M3). One possible explanation for these differences is that the two lifting wires did not become taut at the same moment. The pipe is suspended from two wires which are initially slack, then pulled upwards as the test begins. If the pipe is not lying exactly parallel to the load cell, then one end may be lifted first. The gradient of the initial part of the uplift curve is sensitive to the small strain stiffness of the soil, which is itself very sensitive to strain level. Any 'smearing' of this stiff initial response, due to uneven take up of the slack in the lifting wires, will change the initial slope of the uplift curve. It should be noted that the key measurement, peak uplift, appears to be unaffected by the initial uplift stiffness.

Table 1. Test properties and results

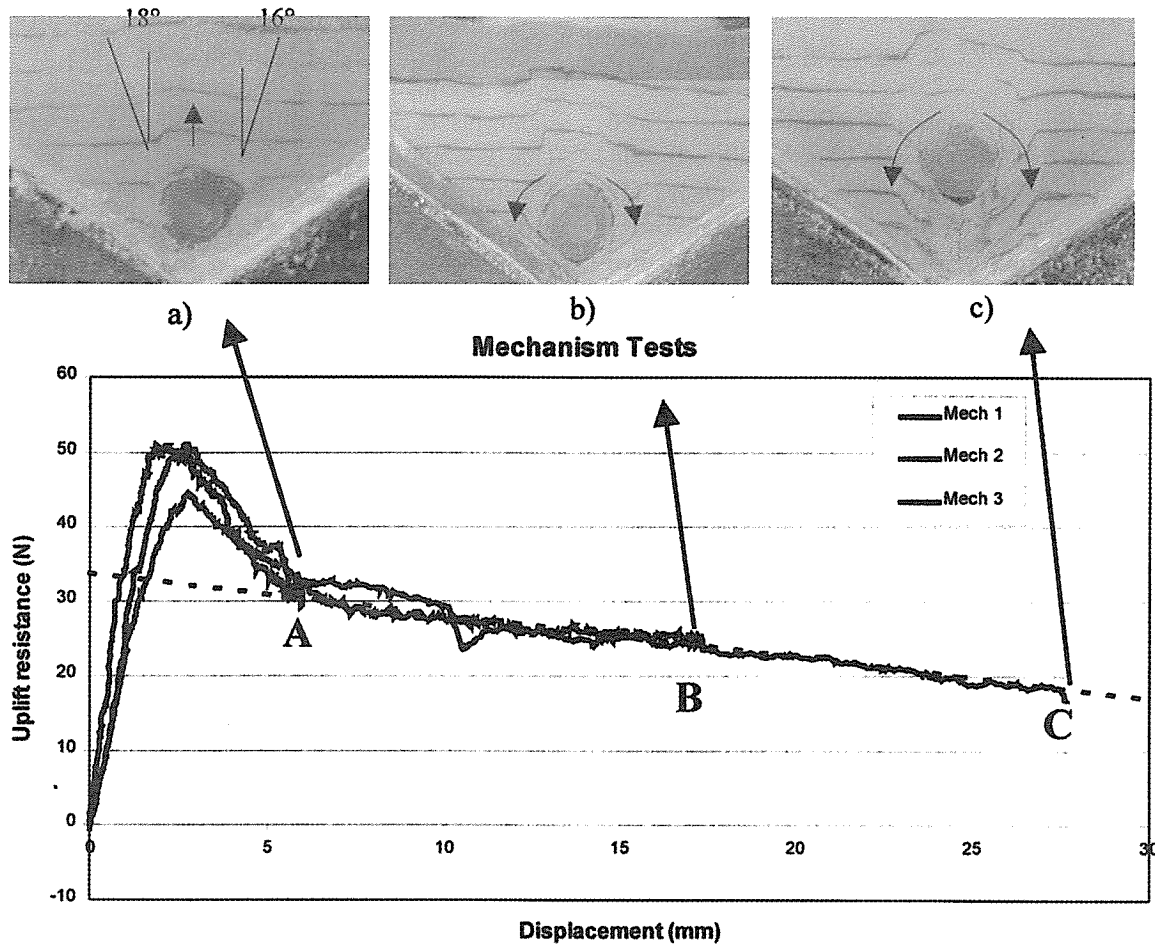| Test	Relative density, I_D	Peak uplift resistance, P (N)	Measured peak uplift factor, F_{up}
M1	44	50	0.66
M2	44	50	0.65
M3	44	44	0.55
L1	22	39	0.49
L2	22	35	0.41
L3	15	40	0.53
L4	22	37	0.45
D1	62	68	0.97
D2	58	50	0.64
D3	62	65	0.91
D4	67	66	0.92
C1	22	36	0.43

Fig. 5. Photography of uplift mechanism

Alternatively, this discrepancy could be attributed to small local variations in sample density (and hence stiffness) close to the pipe, due to the difficulties of preparing a uniform sample around the pre-positioned pipe.

Two modes of deformation are present. During the first stage of uplift, a sliding block mechanism along angled shear planes can be identified. This mechanism is evident in Fig. 5a, and occurs during mobilisation of peak uplift. After further displacement, a 'circulation' mechanism around the pipe periphery is evident (Fig. 5b, 5c). The cavity that forms beneath the pipe during initial uplift is filled by slumping of the surrounding soil.

Two key observations can be made from these photos, and the corresponding uplift curves. Firstly, it is clear that peak uplift resistance is associated with the sliding block mechanism rather than the 'flow' mechanism at this ratio of H/D. Beyond peak uplift, pullout resistance drops by over 50%. Conventional analysis of the failure using a sliding block mechanism (Fig. 1) might lead a designer to assume that the drop in resistance is associated with softening along the shear planes from ϕ_{peak} to ϕ_{crit}. However,

the observed halving of uplift resistance is larger than would be expected for such a change in friction angle. So, a second key observation is that different mechanisms govern the 'peak' and 'residual' stages of the uplift curve.

This raises two questions. Whilst the sliding block mechanism remains the key to predicting peak uplift resistance, the inclination of the slip planes suggests that conventional vertical-sided mechanisms are incorrect. So, firstly, how can the calculation of peak uplift be improved to represent more closely the true failure mechanism? Furthermore, the observation of a circulation mechanism governing the 'residual' part of the uplift curve is puzzling. This failure mechanism offers approximately half the peak resistance provided by the sliding block mechanism. Following ideas of upper bound theory, a designer may be concerned that this apparently 'easy' circulation mechanism may occur during initial uplift, causing a significant reduction in peak resistance. So, secondly, why does a circulation mechanism not occur during initial uplift? The discussion below addresses these two questions.

DISCUSSION

Prediction of peak uplift by improving the sliding block mechanism

It is the sliding block mechanism that must be refined in order to improve the prediction of peak uplift. Examination of Fig. 5a reveals that the failure planes are inclined at 16-18° to the vertical. This change in geometry from the vertical planes shown in Fig. 1 leads to two additional components of uplift resistance: i) the extra weight of soil to be lifted, ii) the change in length and normal stress on the shear planes (Fig. 6).
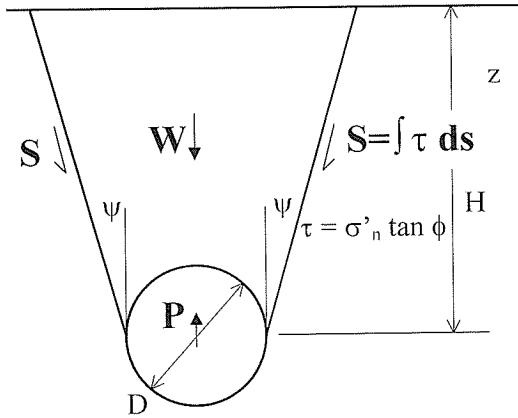
Fig. 6. Sliding block mechanism with shear planes at ψ to the vertical

The angled shear planes are consistent with dilation in the shearing soil. A sawtooth model (Bolton, 1979) may be used to demonstrate the kinematics of dilation. If the shear planes were vertical, a large horizontal stress would be required to suppress dilation, with a corresponding increase in shear stress and hence uplift resistance. A more favourable mechanism is for the shear planes to be inclined at the angle of dilation, ψ, to the vertical. This kinematic arrangement allows the shearing soil to dilate in an unrestrained manner.

The results presented above show that uplift resistance is a strong function of relative density. Also, it is observed that peak uplift is governed by shear planes inclined approximately at ψ to the vertical. These observations are consistent since dilation angle is a function of relative density. This first adjustment of the sliding block mechanism suggests that an improved solution would be of the form:

$$P/\gamma'HD = f(H/D, \phi, K, \psi) \qquad (4)$$

A further adjustment must be made to correct a second anomaly in the sliding block model. A key assumption made in Equation (1) is that the vertical stress along the sliding planes can be found by assuming 'at-rest' conditions. This assumption breaks down close to the pipe crown. The uplift models described in section 2 express the vertical stress at depth z below the ground surface as $\gamma'z$, with the vertical stress on the sliding plane at the pipe being equal to $\gamma'H$. This assumption is fed into the uplift calculation [Equation (2)], which predicts a vertical stress directly above the pipe (P/HD) several times greater than $\gamma'H$, thus contradicting the original assumption.

An alternative distribution of normal stress along the sliding planes must be derived. The 'at-rest' stress conditions of $\sigma_v = \gamma'z$ and $\sigma_h = K_0\gamma'z$ change during the uplift process. A Mohr's circle can be drawn to represent the 'at-rest' conditions, which places the soil within the failure surface (Fig. 7). As uplift occurs, vertical stress is allowed to increase beyond the 'at-rest' value, whilst the normal stress on the sliding plane is assumed to remain unchanged. This new Mohr's circle allows the shear stress on the sliding plane at depth z to be expressed as :

$$\tau = \gamma'z \tan \phi_{peak} [(1 + K_0)/2 - (1 - K_0) (\cos 2\psi)/2] \qquad (5)$$

By integrating along the slip planes and considering the vertical equilibrium of the sliding block, Equation (1) can be rewritten :

$$P = \gamma'HD + \gamma'H^2\tan \psi + \gamma'H^2 (\tan \phi_{peak} - \tan \psi)$$
$$[(1 + K_0)/2 - (1 - K_0)(\cos 2\psi)/2] \qquad (6)$$

This can be normalised into the form of Equation 2, allowing a revised uplift factor, F'_{up} to be derived:

$$F'_{up} = \tan \psi + (\tan \phi_{peak} - \tan \psi)$$
$$[(1 + K_0)/2 - (1 - K_0)(\cos 2\psi)/2] \qquad (7)$$

In order to predict uplift resistance using this revised uplift factor, F'_{up}, a dilation angle must be selected. Bolton (1986) describes a procedure whereby dilation and friction angles are deduced from relative density, ambient stress level, and particle strength.
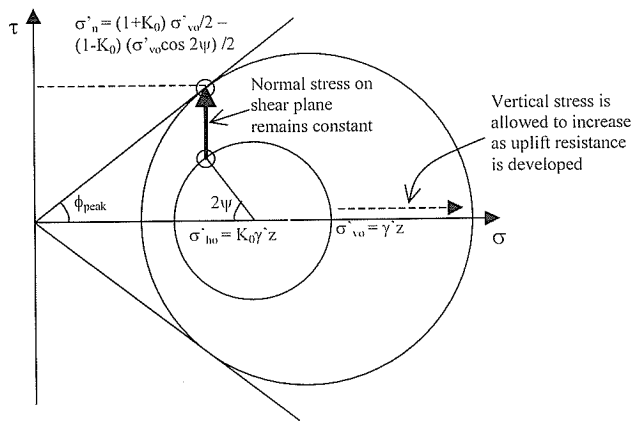
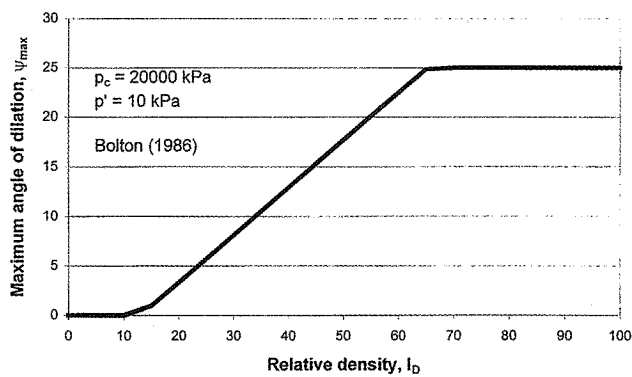Fig. 7. Mohr's circles of soil element on sliding plane

following Bolton (1986). Dilation angle and corresponding values of F'_{up} for each test are shown in Table 2. The at-rest earth pressure coefficient K_0, is taken as 1- $\sin \phi_{crit}$.

The calculated values of F'_{up} correlate closely with the measured values, across the whole range of densities (Fig. 9). The mean value of F'_{up}/F_{up} is 0.93 and the standard deviation is 0.17. In contrast, the empirical guidelines of Schaminee et al. (1990) suggest that F_{up} = 0.4 in sand, which underpredicts the uplift resistance of the dense samples by a factor of 2.3. This data indicates that an analysis based on the dilatant failure mechanism observed during centrifuge testing can provide an improved method for predicting uplift resistance.
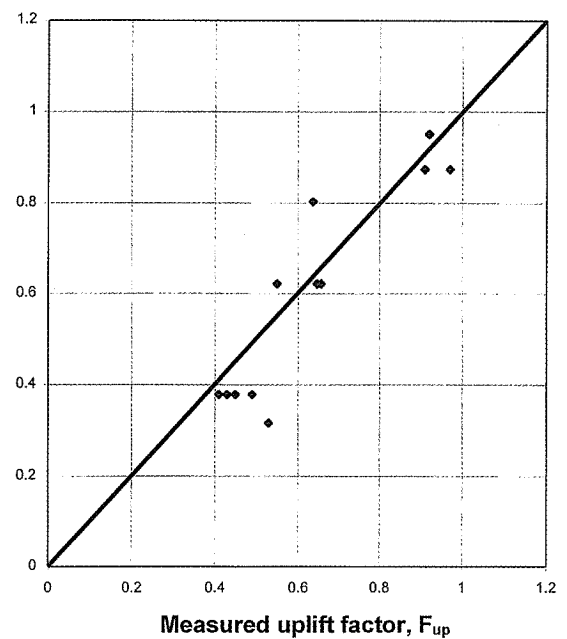

Fig. 8. Relative density, I_D vs. Maximum dilation angle, ψ

Figure 8 shows the relationship between relative density and maximum dilation angle of Fraction D sand at the stress level associated with these tests, which is derived

Predicted uplift factor, F'_{up}

Measured uplift factor, F_{up}

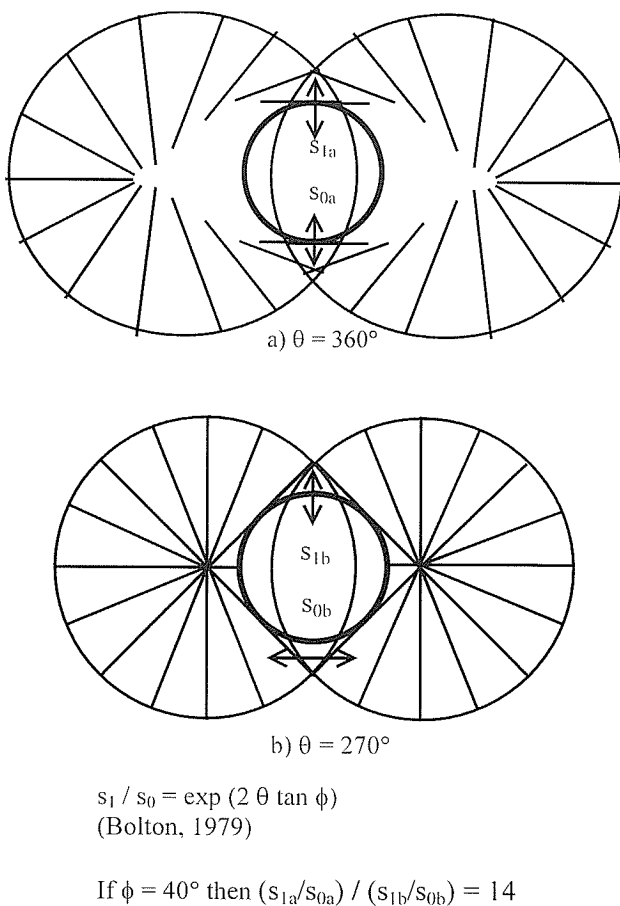Fig. 9. Comparison of predicted and measured uplift factors

Table 2. Dilation angles and revised uplift factors

Test	Relative density, I_D	Maximum dilation angle, ψ_{max}	Calculated uplift Factor, F'_{up}	Measured uplift factor, F_{up}
M1	44	15.0	0.62	0.66
M2	44	15.0	0.62	0.65
M3	44	15.0	0.62	0.55
L1	22	4.4	0.38	0.49
L2	22	4.4	0.38	0.41
L3	16	1.2	0.32	0.53
L4	22	4.4	0.38	0.45
D1	62	23.4	0.87	0.97
D2	58	21.5	0.80	0.64
D3	62	23.5	0.87	0.91
D4	67	25.6	0.95	0.92
C1	22	4.4	0.38	0.43

Mechanism transition associated with the drop from 'peak' to 'residual' uplift

It has been established that peak uplift is well-predicted by a sliding block mechanism based on inclined planes and peak strength. It is tempting to use a similar mechanism to predict the residual uplift resistance, which is observed beyond a displacement of around 1 pipe diameter. However, as shown in Fig. 5, the residual uplift resistance is significantly lower than would be predicted by a reduction in friction angle from peak to residual.

Instead, it is observed that residual uplift is associated with a circulation mechanism in which soil flows around the pipe periphery. At high pipe displacements this circulation mechanism provides a more favourable failure mechanism than the sliding planes. However, why was the apparently 'easier' circulation mechanism not favoured initially? An explanation lies in the change in boundary conditions after a small displacement of the pipe. The initial test condition represents the boundary value problem shown in Fig. 10a. Before any straining has occurred, the major principal stress direction above and below the pipe is vertical. A speculative distribution of slip lines (Bolton, 1979) representing a circulation mechanism is shown. After the pipe has been displaced
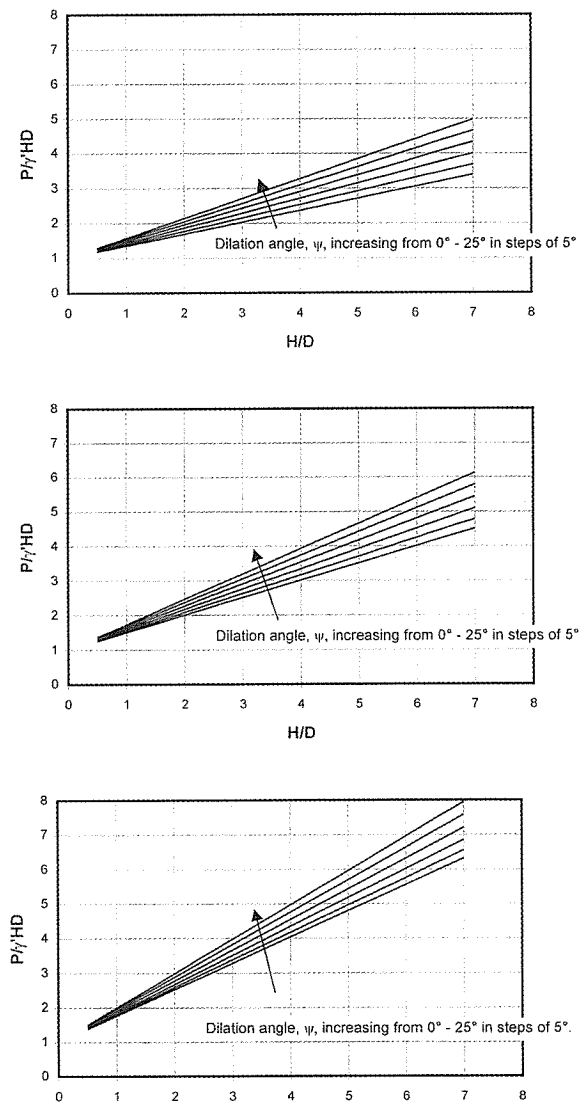
sufficient for a gap to open up beneath the pipe, the boundary conditions change. The problem can now be represented as shown in Fig. 10b, with the major principal stress direction below the pipe being horizontal. The stress rotation associated with the arrangement of slip lines has been reduced by 90 degrees. This corresponds to a reduction in uplift by a factor greater than an order of magnitude.

DESIGN

Using Equation (7) normalised uplift resistance, $P/\gamma'HD$, can be plotted against H/D to demonstrate the influence of dilation angle on uplift resistance (Fig. 11). This envelope of curves encloses all the data shown in Fig. 2 except a few tests in very loose sand at depths of H/D >10. Uplift from deep burial in such loose, contractile material is likely to be associated with a circulation mechanism.

$s_1 / s_0 = \exp(2\theta \tan\phi)$
(Bolton, 1979)

If $\phi = 40°$ then $(s_{1a}/s_{0a}) / (s_{1b}/s_{0b}) = 14$

Fig. 10. **Influence of pipe invert boundary condition on circulation mechanism**

Fig. 11. **Normalised uplift resistance, $P/\gamma'HD$ vs. burial depth, H/D**

Peak uplift resistance is a much stronger function of density than simply the differing weight of loose and dense soil. Whilst a 30% increase in uplift resistance can typically be gained from a 50% increase in burial depth, a similar increase in uplift resistance is associated with a 20% increase in relative density.

The economics of these alternatives may demonstrate that better design and more efficient construction can be achieved through closer attention to the backfilling technique. A construction process which pays close attention to the density of the cover material could lead to a large increase in uplift resistance, or a corresponding reduction in required depth of burial. Ploughing and trench excavation techniques should be optimised to increase the density of the cover material.

Prediction of uplift resistance using Equation (7) requires knowledge of both ψ and ϕ. Also, designers must make an estimate of the relative density of the cover soil. Since ψ is a function of density, grain strength and ambient stress, a suite of laboratory tests are required. Errors in the evaluation of each parameter must be summed.

In contrast, a mini-drum centrifuge model provides a 'one-stop shop' solution. Uplift resistance is calculated directly with only a single laboratory test. The quantity of soil and time required are similar to a triaxial test, and the density of the cover soil can be carefully controlled. If required, the influence of relative density on uplift resistance can be evaluated in a suite of centrifuge tests.

CONCLUSIONS

Reliable prediction of pipe uplift resistance is vital for design against upheaval buckling. Current design methods use a vertical slip model with an empirical uplift factor F_{up}. Recommended values of this empirical factor vary to encompass the density-related spread of published uplift data.

A suite of mini-drum centrifuge tests has been carried out to investigate the mechanism of pipe uplift. It has been observed that peak uplift resistance is associated with a shearing mechanism along planes angled at ψ to the vertical, and that peak resistance is a strong function of density.

An new solution for uplift resistance based on this observed mechanism is presented. The solution shows good correlation with the measured data for a specific burial depth, and addresses some of the inconsistencies of existing design methods. If confirmed over a wider range of burial depths, the resulting design curves will offer improved uplift prediction with reduced empiricism.

These observations demonstrate the strong influence of relative density on uplift resistance. A construction technique that provides a small increase in backfill density can improve uplift resistance as much as a large increase in burial depth.

However, this new design method requires the angle of dilation as an input parameter. A suite of laboratory tests is required to predict dilatancy. Pipe uplift in a mini-drum centrifuge can be considered as an alternative laboratory test, which evaluates uplift resistance directly. Sample density can be carefully controlled, and the influence of density on uplift resistance can be measured directly. Also, whereas the measurement of soil resistance at a stress level of 5-10 kPa is easy in a centrifuge, it is very difficult in a triaxial or shear apparatus.

REFERENCES

1) Barefoot, A.J. (1998): "Modelling the uplift resistance of buried pipes in a drum centrifuge," MPhil thesis, Cambridge University Engineering Department.

2) Barker, H.R. (1999): "Physical modelling of construction processes in the mini-drum centrifuge," Ph.D. thesis, Cambridge University Engineering Department.

3) Bolton, M.D. (1979): "A guide to soil mechanics," M.D. and K. Bolton.

4) Bolton, M.D. (1986): "The strength and dilatancy of sands," Geotechnique, Vol. 36, pp. 65-78.

5) Kulhawy, F.H., Trautmann C. H., Beech J. F., O'Rourke T.D, McGuire W, Wood W. A. and Capano C. (1983): "Transmission line structure foundation for uplift-compression loading," Research Report EL-2870, Electric Power Research Institute, Palo Alto, California.

6) Kvalstad T.J. (1999): "Soil resistance against pipelines in jetted trenches," Proceedings of the Twelfth European Conference on Soil Mechanics and Geotechnical Engineering, Amsterdam Netherlands, Vol. 2, pp. 891-898.

7) Matyas E.L. and Davis J.B. (1983): "Experimental study of earth loads on rigid pipes," ASCE Journal of Geotechnical Engineering, 109 (2) pp. 190-201.

8) Ng C. W. W. and Springman S. M. (1994): "Uplift resistance of buried pipelines in granular materials," Proceedings of Centrifuge '94, Balkema, Rotterdam, Vol. 1, pp. 753-758.

9) Nyman K.J. (1984) : "Soil response against oblique motion of pipes," ASCE Journal of Transportation Engineering, Vol. 110(2), pp. 190-202.

10) Schaminee P.E.L., Zorn N.F., and Schotman G.J.M. (1990): "Soil response for pipeline upheaval buckling analyses: full-scale laboratory tests and modelling," Proceedings of the 22nd Offshore Technology Conference, OTC 6486, pp. 563-572.

11) Schofield A.N. (1998): Geotechnical centrifuge development can correct soil mechanics errors," Proceedings of Centrifuge '98, Balkema, Rotterdam, Vol. 2, pp. 923-930.

12) Spangler M.G. and Handy R.L. (1982): "Soil Engineering," Harper and Row, New York.

13) Stewart D.P., Boyle R.S., and Randolph M.F. (1998): "Experience with a new drum centrifuge," Proceedings of Centrifuge '98, Balkema, Rotterdam, Vol. 1, pp. 35-41.

14) Trautmann C.H., O'Rourke T.D., and Kulhawy F.H. (1985): "Uplift force-displacement response of buried pipe," ASCE Journal of Geotechnical Engineering, 111 (9), pp. 1,061-1,076.